INVITED PAPER *Special Section on Analog Circuit Techniques and Related Topics*

Exact Design of RC Polyphase Filters and Related Issues

Hiroshi TANIMOTO[†a)], ***Member***

SUMMARY This paper presents analysis and design of passive RC polyphase filters (RCPFs) in tutorial style. Single-phase model of a single-stage RCPF is derived, and then, multi-stage RCPFs are analyzed and obtained some restrictions for realizable poles and zeros locations of RCPFs. Exact design methods of RCPFs with equal ripple type, and Butterworth type responses are explained for transfer function design and element value design along with some design examples.

key words: *RC polyphase filters, exact transfer function design, element value design, coefficient matching, cascade synthesis, Butterworth response, equal ripple response*

1. Introduction

An RC polyphase filter (or RCPF, for brevity) is an analog passive filter consisting only of resistors and capacitors, and is well known as a wide band 90° phase splitter. The RCPF is also known for its ability of discriminating positive frequency signals form negative frequency signals of the same frequency. It is needless to say that the RCPFs have been widely used as a basic functional block in wireless telecommunication area, because of those abilities [1], [2].

Polyphase means there are plural sinusoidal signal lines of the same frequency with different phase angles. However, we restrict ourselves to four-phase case in this paper, which is exclusively used in the practical information communication technology.

RCPF is believed to be invented by J.M. Gingell in 1969 as a mean of generating SSB signal easily without using bulky and costly crystal filters [3], [4]. However, RCPF had not been used for long by others.

In 1995, Crols et al. reported possibility of using analog polyphase filters for image rejection in down conversion [5]. The paper itself used an active RC polyphase filter, however, the paper initiated researches toward revival of RCPF, by the author's view. Then, Galal et al. reported that RCPFs are very robust against element value changes [6], and this may attract attention to RCPFs.

The asymmetric frequency response to positive and negative frequency is peculiar to complex constant circuits. Such circuits contain imaginary resistors in addition to usual R, L, C, and may not be realized by conventional passive elements [7]. However, RCPFs are able to realize the asymmetric frequency response with only resistors and capacitors by using polyphase techniques. This is the most remarkable feature of RCPFs and, in addition, they are very suitable for on-chip integration.

There have been many works on RCPF analysis and design [1], [2], [8]–[10], and many RCPFs are actually used, for example, in cellular phones etc. However, most of the designs heavily rely on CAD tools, and it seems that exact design methods of RCPF are known to limited number of specialists, and still remain unknown to public. An exact design makes it possible to provide a prototype quickly for given specifications, and can be served as a starting point of improved designs.

It is the aim of this paper to present exact design methods of RCPFs known to date, in a tutorial way, including the author's observations. The other aim is to point out that there still exists many open problems related such simple RCPF design, in the hope that some of the readers will attack those problems.

2. Analysis of RCPF

2.1 Single Stage Four-Phase RCPF

Inside of the broken line of Fig. 1 shows a well known single-stage four-phase RCPF. The RCPF usually has four voltage driven inputs and its four open terminal voltages of right hand side are used as output voltages.

Usually, the four input voltages are 90° shifted each other. If we take V_{in1} as a reference, the other input voltages are expressed as follows:

$$V_{\text{in2}} = \text{j}V_{\text{in1}}, V_{\text{in3}} = -V_{\text{in1}}, V_{\text{in4}} = -\text{j}V_{\text{in1}}, \tag{1}$$

where j is an imaginary unit. Note that input signals are

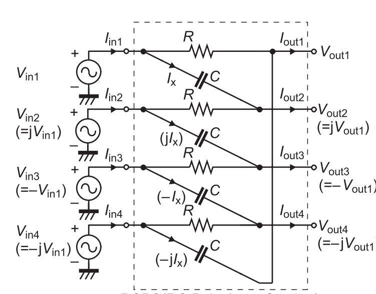

Fig. 1 Single-stage four-phase RCPF (RCPS).

Manuscript received October 9, 2012.
Manuscript revised October 19, 2012.

[†]The author is with the Department of Electrical and Electronic Engineering, Kitami Institute of Technology, Kitami-shi, 090-8507 Japan.
a) E-mail: htanimot@mail.kitami-it.ac.jp

DOI: 10.1587/transfun.E96.A.402

paired as $(V_{\text{in}1}, V_{\text{in}3})$ and $(V_{\text{in}2}, V_{\text{in}4})$ to form two sets of differential quadrature signals, and this fact is friendly to on-chip integration.

From the circular symmetry structure of RCPF, the output voltages also are 90° shifted each other:

$$V_{\text{out}2} = \text{j}V_{\text{out}1}, V_{\text{out}3} = -V_{\text{out}1}, V_{\text{out}4} = -\text{j}V_{\text{out}1}. \tag{2}$$

And so are the currents $I_{\text{in}\,k}$ and $I_{\text{out}\,k}$ $(k = 1, 2, 3, 4)$. In this situation, it suffices to calculate only $V_{\text{in}1}$, $V_{\text{out}1}$, $I_{\text{in}1}$, and $I_{\text{out}1}$, because other voltages and currents are just 90° phase shifted versions of them. This leads to an idea of single-phase representation of the RCPF.

Simple circuit analysis of Fig. 1 gives a single-phase chain matrix $\boldsymbol{F}$ of the single-stage RCPF as

$$\begin{pmatrix} V_{\text{in}1} \\ I_{\text{in}1} \end{pmatrix} = \underbrace{\frac{1}{1 - \text{j}sCR} \begin{pmatrix} 1 + sCR & R \\ 2sC & 1 + sCR \end{pmatrix}}_{\equiv \boldsymbol{F}} \begin{pmatrix} V_{\text{out}1} \\ I_{\text{out}1} \end{pmatrix}. \tag{3}$$

This $\boldsymbol{F}$ can also be represented as Eq. (4) by introducing time constant of the stage, $\tau \equiv RC$.

$$\boldsymbol{F} = \frac{1}{1 - \text{j}s\tau} \begin{pmatrix} 1 + s\tau & R \\ 2sC & 1 + s\tau \end{pmatrix} \tag{4}$$

By using standard cascade matrix to admittance matrix conversion, we have a single-phase equivalent admittance matrix $\boldsymbol{Y}$ of a single-stage RCPF as:

$$\boldsymbol{Y} = \begin{pmatrix} G(1 + s\tau) & -G(1 + \text{j}s\tau) \\ -G(1 - \text{j}s\tau) & G(1 + s\tau) \end{pmatrix}, \tag{5}$$

here, $G = 1/R$. Note that $\boldsymbol{Y}$ is solely characterized by G and τ. Equation (5) indicates that $y_{12}(s) \neq y_{21}(s)$, and that RCPF is a non-reciprocal circuit.

2.2 Frequency Response of Single-Stage RCPF

Voltage transfer function of a single-stage RCPF is analyzed next. Let $T(s)$ be voltage transfer function of a single-stage RCPF. $T(s)$ is given by a reciprocal of $(1, 1)$ component of the matrix $\boldsymbol{F}$:

$$T(s) = \frac{V_{\text{out}1}}{V_{\text{in}1}} = \frac{1 - \text{j}s\tau}{1 + s\tau}. \tag{6}$$

The numerator polynomial has a coefficient of complex number; hence, RCPF belongs to complex constant circuits. Putting $s = \text{j}\omega$ in (6), magnitude response of RCPF is plotted as in Fig. 2 for $\tau = 1$.

Note that the magnitude response is not symmetrical about $\omega = 0$, and has a broad peak at $\omega = +1$, has a narrow notch at $\omega = -1$. This is the particular nature of RCPF response differentiating from usual real filters.

The implication of *negative* frequency is as follows. Suppose the sequence of input voltages for positive ω is

$$V_{\text{in}\,k}(t) = V\cos(\omega t + k\pi/2), \quad (k = 0, 1, 2, 3) \tag{7}$$

If ω is replaced with $-\omega$ in the above input voltages, then

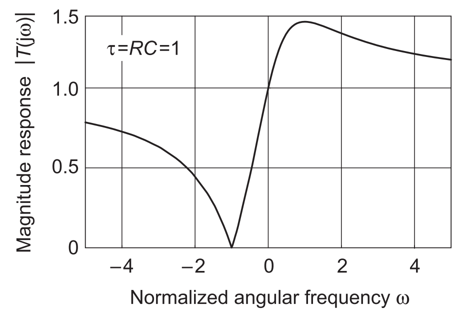

Fig. 2 Magnitude response of RCPF.

the following relations hold:

$$\begin{aligned} V_{\text{in}\,k}(t) &= V\cos(-\omega t + k\pi/2) \\ &= V\cos(\omega t - k\pi/2), \quad (k = 0, 1, 2, 3) \end{aligned} \tag{8}$$

Hence, positive frequency corresponds to signals with a phase angle sequence of $(0, \pi/2, \pi, 3\pi/2)$, and negative frequency to a sequence of $(0, -\pi/2, -\pi, -3\pi/2)$. Traditionally, the former sequence is called *negative sequence*, and the latter is *positive sequence*, in the polyphase terminology [11]. So, the positive or negative frequency represents only wiring order of quadrature phase signals. In other words, RCPF can distinguish positive sequence from negative sequence.

2.3 Frequency Response of Multi-Stage RCPF

Now, if a wider notch, or stopband, is needed, we usually cascade several single-stage RCPFs, then, we have a multi-stage RCPF. Equation (6) indicates that its zero and pole frequencies have the same magnitude. This fact restrict our design freedom, if we are cascading N single-stage RCPFs with buffer amplifiers in between them (Fig. 3(a)). Resulting voltage transfer function will have following form.

$$T_{\text{buffered}}(s) = A \prod_{k=1}^{N} \frac{1 - \text{j}s\tau_k}{1 + s\tau_k}, \tag{9}$$

where, τ_k $(k = 1, 2, \ldots, N)$ indicates a time constant of the k-th RCPF stage, and A is a gain at dc. Equation (9) means that once we specify locations of zero, pole locations will automatically be determined and cannot be controlled. This also means that we have to add some equalizing filter to obtain a flat passband.

In turn, if the buffers are removed and single-stage RCPFs are directly cascaded (Fig. 3(b)), zeros will remain unchanged before cascading, and poles will shift their location. This suggests there exist some possibility of controlling pole location without changing zero location; however, this will raise another difficult design problem. Those are the next issues.

To see what is like a directly cascaded multi-stage RCPF response, cascade matrix of a single-stage RCPF is useful. Let N be a number of cascaded stages, and assume the k-th stage has chain matrix $\boldsymbol{F}_k$, where $k = 1, 2, \ldots, N$. Each $\boldsymbol{F}_k$ is characterized by its own time constant $\tau_k = R_k C_k$.

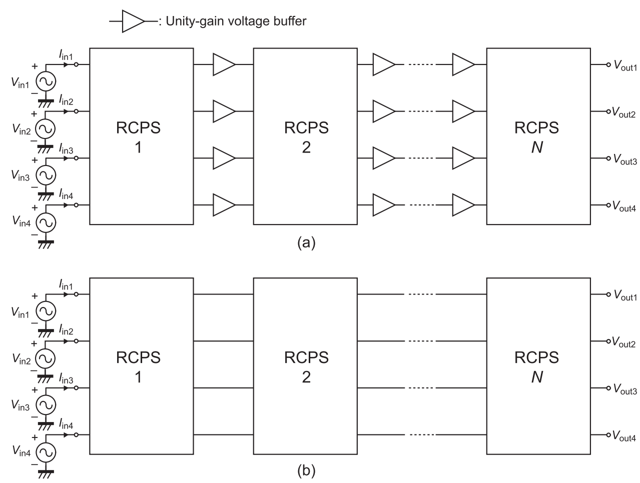

Fig. 3 Multi-stage RCPF with (a), and without (b) interstage voltage-buffers.

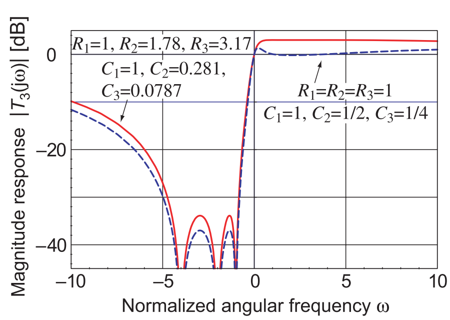

Fig. 4 Example magnitude response of 3-stage RCPF.

Then, the total chain matrix of the cascaded RCPF will be of the form

$$\begin{aligned}\boldsymbol{F}_{\text{total}} &= \boldsymbol{F}_1\boldsymbol{F}_2\cdots\boldsymbol{F}_N\\ &= \prod_{k=1}^{N}\frac{1}{1-\mathrm{j}s\tau_k}\begin{pmatrix}1+s\tau_k & R_k\\ 2sC_k & 1+s\tau_k\end{pmatrix}\\ &= \begin{pmatrix}A(s) & B(s)\\ C(s) & D(s)\end{pmatrix}\prod_{k=1}^{N}\frac{1}{1-\mathrm{j}s\tau_k},\end{aligned} \tag{10}$$

where $A(s), C(s), D(s)$ are N-th order polynomials of s and $B(s)$ is a $(N-1)$-st order polynomial. Then, voltage transfer function of N-stage RCPF, $T_N(s)$, has the following form:

$$T_N(s) = \frac{(1-\mathrm{j}s\tau_1)(1-\mathrm{j}s\tau_2)\ldots(1-\mathrm{j}s\tau_N)}{A(s)} \tag{11}$$

Because this is a transfer function of an *RC* circuit, its denominator must have only negative real poles. So, by introducing pole time constants $\tau_k^{[\mathrm{p}]} > 0$ $(k = 1, 2, \ldots, N)$, and renaming τ_k to $\tau_k^{[\mathrm{z}]}$ for avoiding confusion, we have

$$T_N(s) = \frac{(1-\mathrm{j}s\tau_1^{[\mathrm{z}]})(1-\mathrm{j}s\tau_2^{[\mathrm{z}]})\ldots(1-\mathrm{j}s\tau_N^{[\mathrm{z}]})}{(1+s\tau_1^{[\mathrm{p}]})(1+s\tau_2^{[\mathrm{p}]})\ldots(1+s\tau_N^{[\mathrm{p}]})}. \tag{12}$$

Figure 4 compares two design examples for magnitude response of 3-stage RCPF. Both design have the same zero time constants, but have different pole time constants.

Table 1 Element values for two different designs with the same zeros.

k	R_k	C_k	$\tau_k{}^{[p]}$	R'_k	C'_k	$\tau_k{}^{[p]'}$
1	1 Ω	1 F	0.0788	1 Ω	1 F	0.117
2	1 Ω	1/2 F	0.5	1.78 Ω	0.281 F	0.5
3	1 Ω	1/4 F	3.171	3.17 Ω	0.0787 F	2.132

Element values for each stage and calculated time constants for zeros and poles are summarized in Table 1. We clearly see three notches for both designs at $\omega = -1, -2, -4$ as expected from time constants of zeros. However, to know pole location, we need some cumbersome calculations. The results are also shown in Table 1 in ascending order of magnitude.

3. Transfer Function Design for RC Polyphase Filters

Systematic design methodology is not very popular; however, many designs have been made with intensive use of circuit simulation. So, the most popular method may be cut-and-try method. Other two methods, i.e., direct design method and frequency transform method are explained in the following sections, after a short visit to cut-and-try method.

From the preceding analysis, the voltage transfer function of an RCPF is represented in the following form by rewriting Eq. (12) as

$$\begin{aligned}H(s) &= \frac{(1-s/z_1)(1-s/z_2)\ldots(1-s/z_N)}{(1-s/p_1)(1-s/p_2)\ldots(1-s/p_N)}\\ &= \frac{(s-z_1)(s-z_2)\ldots(s-z_N)}{(s-p_1)(s-p_2)\ldots(s-p_N)}\frac{p_1p_2\ldots p_N}{z_1z_2\ldots z_N},\end{aligned} \tag{13}$$

with poles $p_k = -1/\tau_k^{[\mathrm{p}]}$, and zeros $z_k = -\mathrm{j}/\tau_k^{[\mathrm{z}]}$ for $k = 1, 2, 3, \ldots, N$. Also, $H(0) = 1$ holds automatically.

Capacitors are short circuited at very high frequency, and they connect to next line with circular symmetry, so that N stage RCPF behaves just like a phase rotator of $\mathrm{e}^{\mathrm{j}N\pi/2}$ at $s = \mathrm{j}\infty$. Then,

$$\frac{p_1p_2\ldots p_N}{z_1z_2\ldots z_N} = \mathrm{e}^{\mathrm{j}N\pi/2}, \text{ or } \frac{\tau_1^{[\mathrm{z}]}\tau_2^{[\mathrm{z}]}\ldots\tau_N^{[\mathrm{z}]}}{\tau_1^{[\mathrm{p}]}\tau_2^{[\mathrm{p}]}\ldots\tau_N^{[\mathrm{p}]}} = 1 \tag{14}$$

holds.

Note that even we may design any transfer function if the poles and zeros will not violate the physical realizability condition, however, we must restrict ourselves to use only RCPF structure to realize the transfer function.

To summarize, the *necessary conditions* for a voltage transfer function $H(s)$ to be realized in a cascaded RC-polyphase sections are:

1. All poles of $H(s)$ are on the negative real axis,
2. All zeros of $H(s)$ are on the negative imaginary axis,
3. $H(0) = 1$ and $\prod_{k=1}^{N}\left(\tau_k^{[\mathrm{z}]}/\tau_k^{[\mathrm{p}]}\right) = 1$ holds.

Unfortunately, *sufficient conditions* are not known to date.

It is very easy to specify attenuation poles, i.e., zeros of the transfer function, because they solely determined by the time constants of each section. However, the same time constants interferes each other to make up pole location. This is the biggest problem if one wished to have, say, equal ripple passband. If the number of stages is small, numerical optimization may be used, however, it is difficult for higher order RCPFs. So, we need some analytic methods to design like traditional Butterworth or equal ripple designs.

3.1 Direct Design Method

The equal-ripple design method was found first in 1975. Gingell derived and solved a differential equation to obtain simultaneously equal ripple within its passband and stop band for RCPF [4], in a similar way to elliptic LPF design as described in reference [20], and derived an analytic expression for the voltage transfer function of equal ripple RCPFs. He also proved that its poles and zeros must lie on the negative real axis and imaginary axis, respectively, so that they can be expressed by time constants like Eq. (12) [4].

An equal ripple RCPF can be characterized by three parameters N, x, and ε. Here, N is a number of RC polyphase filter sections and is equal to the order of the RCPF, x is a square root of a relative bandwidth defined by $x \equiv \sqrt{\omega_L/\omega_H}$ (< 1), where ω_L and ω_H are angular frequencies of lower edge and higher edge of passband and/or stopband, respectively. ε is a ripple parameter, and is related to passband ripple, A_p, and stopband attenuation, A_s, via the relations

$$A_p = 10\log_{10}(1+\varepsilon^2)\ \ [\mathrm{dB}] \tag{15}$$

and

$$A_s = 10\log_{10}(1+1/\varepsilon^2)\ \ [\mathrm{dB}]. \tag{16}$$

Among the above three parameters, N, x, ε, only two can be independently specified, and the rest is determined automatically. The constraint among them is given by [4]

$$4N\frac{K(x^2)}{K(\sqrt{1-x^4})} = \frac{K(\sqrt{1-\varepsilon^4})}{K(\varepsilon^2)}, \tag{17}$$

where, $K(k)$ is the complete elliptic integral of the first kind with k as a modulus [21]. For example, if N and x are given, then ε can be determined by solving Eq. (17) for ε.

Figure 5 shows this constraint for $N = 1$ to 14, and is useful to find a required number of sections, N, for a given bandwidth and A_s or A_p. For a fixed N, stopband attenuation decreases with relative bandwidth ω_H/ω_L. Note that A_p becomes very small for $A_s > 20$ dB and gives very flat passband.

The voltage transfer function of the RC polyphase filter having equal ripple property both in stopband and passband is given by [4]:

$$H(s)=\prod_{r=1}^{N}\frac{s+\mathrm{j}\,\frac{1}{x}\,\mathrm{dn}\left[\left(\frac{2r-1}{2N}\right)K\left(\sqrt{1-x^4}\right),\ \sqrt{1-x^4}\right]}{s+\frac{1}{x}\,\mathrm{cs}\left[\left(\frac{2r-1}{2N}\right)K\left(\sqrt{1-x^4}\right),\ \sqrt{1-x^4}\right]}, \tag{18}$$

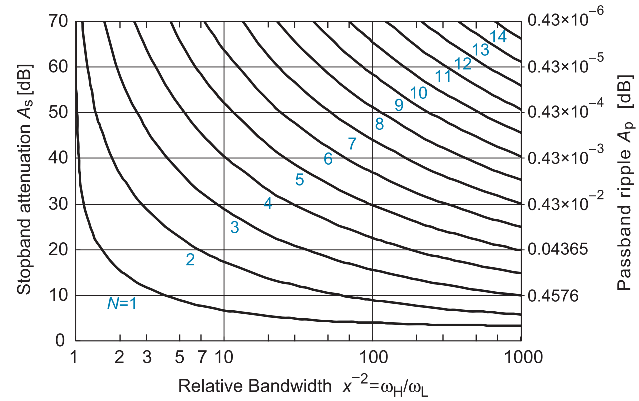

Fig. 5 Relation between number of sections, attenuation and bandwidth.

where, $\mathrm{dn}(u,k)$ and $\mathrm{cs}(u,k)$ are Jacobian elliptic functions with variable u and modulus k [21].

Equation (18) can be factorized in the following form:

$$H(s) = \frac{(1-\mathrm{j}s\tau_1^{[z]})(1-\mathrm{j}s\tau_2^{[z]})\cdots(1-\mathrm{j}s\tau_N^{[z]})}{(1+s\tau_1^{[p]})(1+s\tau_2^{[p]})\cdots(1+s\tau_N^{[p]})} \tag{19}$$

where, time constants are explicitly given by

$$\tau_r^{[z]} = \frac{1}{x}\mathrm{dn}\left[\left(\frac{2r-1}{2N}\right)K\left(\sqrt{1-x^4}\right),\ \sqrt{1-x^4}\right], \tag{20}$$

$$\tau_r^{[p]} = \frac{1}{x}\mathrm{cs}\left[\left(\frac{2r-1}{2N}\right)K\left(\sqrt{1-x^4}\right),\ \sqrt{1-x^4}\right], \tag{21}$$

for $r = 1, 2, 3, \ldots, N$. Thus, it is convenient to number them in descending order of magnitude as

$$\tau_1^{[z]} > \tau_2^{[z]} > \cdots > \tau_{N-1}^{[z]} > \tau_N^{[z]}, \tag{22}$$

$$\tau_1^{[p]} > \tau_2^{[p]} > \cdots > \tau_{N-1}^{[p]} > \tau_N^{[p]}, \tag{23}$$

where, $p_r = -1/\tau_r^{[p]}, z_r = -\mathrm{j}/\tau_r^{[z]}$ $(r = 1, 2, \ldots, N)$.

It should be noted that for normalized design that the following symmetry relations between the time constants hold. For odd integer N,

$$\tau_1^{[p]}\tau_N^{[p]} = \tau_2^{[p]}\tau_{N-1}^{[p]} = \cdots = \tau_{\frac{N+1}{2}}^{[p]\ 2} = 1, \tag{24}$$

$$\tau_1^{[z]}\tau_N^{[z]} = \tau_2^{[z]}\tau_{N-1}^{[z]} = \cdots = \tau_{\frac{N+1}{2}}^{[z]\ 2} = 1, \tag{25}$$

and, for even integer N,

$$\tau_1^{[p]}\tau_N^{[p]} = \tau_2^{[p]}\tau_{N-1}^{[p]} = \cdots = \tau_{\frac{N-1}{2}}^{[p]}\tau_{\frac{N+1}{2}}^{[p]} = 1, \tag{26}$$

$$\tau_1^{[z]}\tau_N^{[z]} = \tau_2^{[z]}\tau_{N-1}^{[z]} = \cdots = \tau_{\frac{N-1}{2}}^{[z]}\tau_{\frac{N+1}{2}}^{[z]} = 1, \tag{27}$$

hold by the property of elliptic functions [22]. Then, $H(0) = 1$ and $\prod_{k=1}^{N}\left(\tau_k^{[z]}/\tau_k^{[p]}\right) = 1$ hold, and the method gives transfer functions which satisfy the necessary conditions to be realized in cascaded RCPF sections.

A normalized pole/zero table is found in reference [4] compiled for $N = 2$ to 9 and stopband attenuation from 35 dB to 70 dB in steps of 5 dB.

Table 2 Pole/zero locations for design example 1.

#	Poles	Zeros
1	−0.242623	−j0.551712
2	−1.000000	−j1.000000
3	−4.121629	−j1.812540

(1) *Design example 1*: Third order equal ripple RCPF

Suppose we design a transfer function of normalized equal ripple RCPF with $\omega_L = 0.5$, $\omega_H = 2.0$, i.e., $x = 0.5$, and $A_s > 40$ dB. Form Fig. 5, we need $N \geqq 3$ to obtain $A_s > 40$ dB, then, $N = 3$ is chosen. The ripple parameter ε can be determined as $\varepsilon = 0.009302$ by solving Eq. (17) numerically. This leads to passband and stopband ripples to be $A_p = 0.00037577$ dB, and $A_s = 40.628$ dB. From these values, poles and zeros are calculated by using Eqs. (20) and (21) as listed in Table 2.

3.2 Frequency Transformation Methods for RCPF

Bilinear frequency transformation has been used to obtain voltage transfer function of a complex filter from symmetric real lowpass prototype [4], [12], [13].

However, this frequency transformation must be tailored for use with RCPFs, because RCPFs belong to a subclass of general analog complex filters, and thus, a transfer function of RCPF must have its poles on the negative real axis, and zeros on the imaginary axis. Considering these facts, Muto and Hori independently pointed out that the prototype normalized symmetric lowpass filter must meet the conditions [14], [15]:

1. The prototype lowpass filter must have its poles all on a unit circle.
2. The prototype lowpass filter must have its zeros all on imaginary axis.

Let target RCPF's passband be (ω_L, ω_H), and their geometric mean be $\omega_0 = \sqrt{\omega_L \omega_H}$, and they are normalized in such a way that $\omega_0 = 1$ holds. The stopband is assumed to be $(-\omega_H, -\omega_L)$. Also, the prototype lowpass filter is assumed to have a passband edge at Ω_p and a stopband edge at Ω_s, with them normalized as $\Omega_p \Omega_s = 1$.

From these constraints, they obtained suitable bilinear transformation [14], [15] to be

$$\lambda = \mathrm{j}\,\frac{s - \mathrm{j}}{s + \mathrm{j}}, \quad \text{or} \quad s = -\mathrm{j}\,\frac{\lambda + \mathrm{j}}{\lambda - \mathrm{j}}, \tag{28}$$

where $\lambda (= \mathrm{j}\Omega)$ is a normalized complex frequency variable of the prototype LPF, and $s (= \mathrm{j}\omega)$ is a normalized complex frequency variable of the target RCPF.

The latter bilinear transformation maps $\lambda = u + \mathrm{j}v$ onto

$$s = \frac{2u}{u^2 + (v-1)^2} - \mathrm{j}\,\frac{u^2 + v^2 - 1}{u^2 + (v-1)^2}. \tag{29}$$

This clearly indicates that the unit circle on λ-plain, $u^2 + v^2 = 1$, maps onto real axis, and if $u < 0$, this maps onto negative real axis. In addition, the imaginary axis of λ-plain, $u = 0$, maps onto the imaginary axis of the s-plain. Also, negative real axis, $u < 0$ and $v = 0$, maps onto left-half of the s-plain. Figure 6 shows the mapping from λ-plain to s-plain.

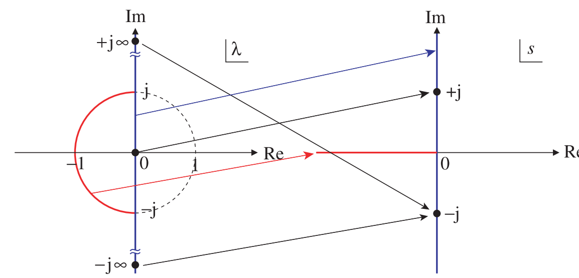

Fig. 6 Bilinear mapping from λ-plain to s-plain.

Among well known real filters, only Butterworth LPFs and Elliptic LPFs of the Zolotarev type have the above two properties [14], [15]. Butterworth type RCPF was first introduced by those references.

Now, this seems everything goes well; however, two points must be taken care of. First, the issue of phase shift at dc. The transform of Eq. (28) maps the origin $\lambda = 0$ to $s = \mathrm{j}$. This implies that the mapped transfer function may exhibit phase shift even at dc and this is physically unacceptable for RCPF. This is the direct consequence of shifting the passband having negative to positive frequency range $\Omega \in (-\Omega_p, +\Omega_p)$ to a positive passband $\omega \in (\omega_L, \omega_H)$. Notwithstanding this fact, the transform gives correct poles and zeros, and is still useful. A simple remedy for this issue is to renormalize the gain factor to have unity gain at dc [15], or use only transformed poles and zeros [14].

Another issue need to be considered is the *frequency warping effect* as in the well known case of digital filter design with bilinear s-z transform [17]. The bilinear transform in Eq. (28) maps the original stopband $|\Omega| > \Omega_s$ into $\omega \in (-\omega_H, -\omega_L)$, the original Ω_p and Ω_s must be prewarped to Ω'_p and Ω'_s in such a way that

$$\Omega'_p = -\frac{1 - \omega_H}{1 + \omega_H}, \quad \Omega'_s = \frac{1 - \omega_L}{1 + \omega_L} \tag{30}$$

are satisfied. We must design the prototype with prewarped relative bandwidth $\kappa = \Omega'_p / \Omega'_s$.

Hence, before and after transforming the prototype function, we take care for the following:

1. The prototype lowpass filter's passband/stopband edges are prewarped to have desired RCPF's passband/stopband edges as Eq. (30).
2. Obtained RCPF transfer function via Eq. (28) have to be normalized to have a unity gain at dc.

Those will be explained in the examples.

3.2.1 Transfer Function Design of Butterworth RCPF

As is well known, a normalized N-th order Butterworth LPF has the transfer function $H(\lambda)$ of the following form:

$$H(\lambda) = \frac{1}{(\lambda-\lambda_1)(\lambda-\lambda_2)\ldots(\lambda-\lambda_N)}, \tag{31}$$

$$\lambda_k = \mathrm{e}^{\mathrm{j}\frac{(2k+N-1)\pi}{2N}} \quad (k = 1, 2, 3, \ldots, N). \tag{32}$$

Applying the bilinear λ to s transform of Eq. (28) to a single pole of Eq. (31), we have

$$\frac{1}{\lambda-\lambda_k} \rightarrow \frac{-\mathrm{j}(s+\mathrm{j})}{s(1+\mathrm{j}\lambda_k)-(\lambda_k+\mathrm{j})} \tag{33}$$

This means that each pole maps to a negative real pole and a zero at $s = -\mathrm{j}$, so that there will be N-fold zero at $s = -\mathrm{j}$ as a factor of $(1-\mathrm{j}s)^N$. This is a suitable function when a very deep notch is required.

(1) Design example 2: First-order Butterworth RCPF

The voltage transfer function of prototype LPF is given by:

$$H_1(\lambda) = \frac{1}{\lambda+1} \tag{34}$$

Applying the bilinear λ to s transform of Eq. (28) to Eq. (34), we have

$$H_1\left(\mathrm{j}\frac{s-\mathrm{j}}{s+\mathrm{j}}\right) = \frac{\mathrm{j}}{1+\mathrm{j}}\,\frac{1-\mathrm{j}s}{1+s}. \tag{35}$$

Comparing this and Eq. (6) with $\tau = 1$, Eq. (35) has an extra gain constant of $\mathrm{j}/(1+\mathrm{j})$. We renormalize Eq. (35) so that it has a unity gain at $s = 0$. The result is

$$H_{\mathrm{RCPF1}}(s) = \frac{1-\mathrm{j}s}{1+s}. \tag{36}$$

This is exactly the same as Eq. (6) and what is shown in Fig. 2.

(2) Design example 3: Third-order Butterworth RCPF

The prototype LPF transfer function $H_3(\lambda)$ is given by

$$H_3(\lambda) = \frac{1}{(\lambda+1)(\lambda^2+\lambda+1)}. \tag{37}$$

This maps to

$$H_3\left(\mathrm{j}\frac{s-\mathrm{j}}{s+\mathrm{j}}\right) = -\frac{1+\mathrm{j}}{2}\,\frac{(s+\mathrm{j})^3}{s^3+5s^2+5s+1}. \tag{38}$$

After renormalizing to have unity gain at dc, we have

$$H_{\mathrm{RCPF3}}(s) = \frac{(1-\mathrm{j}s)^3}{(1+s)\left(1+\dfrac{s}{2-\sqrt{3}}\right)\left(1+\dfrac{s}{2+\sqrt{3}}\right)}. \tag{39}$$

This clearly shows existence of triple zero at $\omega = -1$, and is specific to the transfer functions derived from Butterworth filters.

3.2.2 Transfer Function Design of Elliptic RCPF

In the usual elliptic LPF design, only three parameters can be independently specified among the four parameters of A_p the maximum passband attenuation, A_s the minimum stopband attenuation, the separation factor $\kappa = \Omega_\mathrm{p}/\Omega_\mathrm{s}$, and a filter order N. Then, the discrimination factor $k_1 = \sqrt{\frac{10^{A_\mathrm{p}/10}-1}{10^{A_\mathrm{s}/10}-1}}$ is determined. This means we have some freedom trading A_p for A_s, and the fact is utilized in elliptic LPF design [16]. However, we must give this up and introduce the following constraint to obtain the Zolotarev filter response, which has poles solely located on the unit circle [15]:

$$10^{A_\mathrm{p}/10} = \frac{10^{A_\mathrm{s}/10}}{10^{A_\mathrm{s}/10}-1}, \quad \text{i.e.,} \quad k_1 = \frac{1}{10^{A_\mathrm{s}/10}-1} \tag{40}$$

The N-th order normalized elliptic LPFs have following transfer functions:

$$H(\lambda) = \frac{H_0}{\lambda+1}\prod_{k=1}^{(N-1)/2}\frac{(\lambda+z_k)^2}{(\lambda+p_k)(\lambda+p_k^*)} \quad \text{for odd } N, \tag{41}$$

$$= H_0\prod_{k=1}^{N/2}\frac{(\lambda+z_k)^2}{(\lambda+p_k)(\lambda+p_k^*)} \quad \text{for even } N, \tag{42}$$

where, H_0 is a gain constant, p_k and p_k^* $(k = 1, 2, \ldots, [N/2])$ are complex conjugate pair of k-th poles, and z_k $(k = 1, 2, \ldots, [N/2])$ are zeros on the imaginary axis. The poles must be on the unit circle. Such poles and zeros of Zolotarev type LPF can be found in design tables [16], or directly calculated by using software [18].

(1) Design example 4: Third-order elliptic RCPF

First we design an $N = 3$ normalized elliptic LPF with $\Omega_\mathrm{p} = 0.5$, $\Omega_\mathrm{s} = 2.0$, i.e., $\kappa \equiv \Omega_\mathrm{p}/\Omega_\mathrm{s} = 1/4^\dagger$. Analytical expression relating κ, k_1, and N to have the elliptic response is found in Ref. [19]. For $N = 3$ case, the expression is

$$k_1 = \kappa^3 \mathrm{cd}\left(\frac{2}{3}K(\kappa), \sqrt{\kappa}\right)^4\Bigg|_{\kappa=1/4} = 0.00102469, \tag{43}$$

where $\mathrm{cd}(u, k)$ is a Jacobian elliptic function with variable u and modulus k, and $K(k)$ is a complete elliptic integral of the first kind. From this k_1 value and Eq. (40), we have

$$A_\mathrm{s} = 29.8985\,[\mathrm{dB}], \quad A_\mathrm{p} = 0.00444791\,[\mathrm{dB}]. \tag{44}$$

For those values of $N, \Omega_\mathrm{p}, A_\mathrm{p}$, we can calculate normalized poles and zeros by using any standard CAD tool, and are listed on Table 3, with resulting normalized RCPF poles and zeros by using the transform of Eq. (28) with $\omega_0 = 1$. Figure 7 shows its magnitude response of the transformed RCPF.

The transformed RCPF transfer function has a stopband of $(-3.000, -0.3333)$, and is not $(-2, -0.5)$. This can be explained by the frequency warping effect. We specified $\Omega_\mathrm{p} = 0.5$ and $\Omega_\mathrm{s} = 2.0$. Then, $\Omega_\mathrm{p} = 0.5$ maps to $\omega = 3.0$, while $-\Omega_\mathrm{p} = -0.5$ maps to $\omega = 0.3333$. So, if we specified $\Omega'_\mathrm{p} = 0.3333$ and $\Omega'_\mathrm{s} = 3.0$ instead, we could have obtained the RCPF transfer function with a stopband of $(-2.0, -0.5)$.

$^\dagger\kappa$ is a reciprocal of often used *selectivity factor* ξ.

Table 3 Poles and zeros of prototype LPF and transformed RCPF.

		Prototype LPF	Transformed RCPF
Pole #1	p_1	−1.00000	−1.00000
#2	p_2	−0.405498−j0.914096	−0.211848
#3	p_3	−0.405498+j0.914096	−4.72035
Zero #1	z_1	−j2.3002	−j0.393976
#2	z_2	+j2.3002	−j2.53823
#3	z_3	±j∞	−j

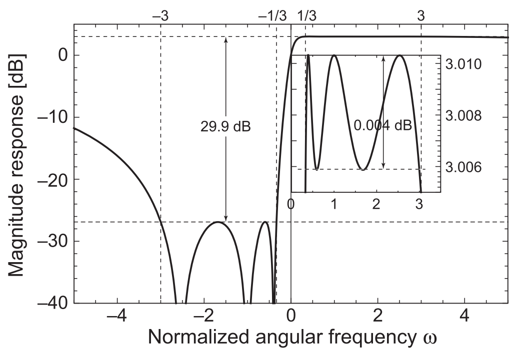

Fig. 7 Magnitude response of transformed equal ripple RCPF.

4. Element Value Design

Voltage transfer functions for RCPFs are obtained so far, the next issue is to obtain *RC* values that realize the desired transfer function. Surprisingly, this is not fully solved to date. This may be a fundamental reason why designers rely heavily upon circuit simulators. Hence, the most popular method to obtain element values of an RCPF is numerical one; however, there are some efforts toward analytic way. This section explains numerical methods first, and then, refer to a cascade synthesis method for RCPF.

4.1 Numerical Design Methods

Since we know the transfer functions obtained both from the actual circuits like Eq. (12), and from pole/zero placement for physically realizable *RC* circuit like Eq. (18). By equating them, we obtain nonlinear simultaneous equations for *RC* values and pole/zero values.

This leads to a classical coefficient matching problem; however, it was very hard to solve the problem in 1970's when computer power was poor [4], and such attempt was not seen until recently.

In 2003, Wada et al. attacked this problem by using numerical optimization [22], [23]. They assumed symmetry property† in the equal ripple RCPFs and could reduced the number of unknown parameters. This resulted in good numerical convergence; however, the resulted *RC* values gave only approximately realize the original transfer function and is suboptimal, i.e., the number of passband ripple is reduced, and the ripple becomes larger, than expected from the transfer function [24]. Actually, the change in passband ripple is very small and negligible for many practical uses.

Tanabe et al. coped with this coefficient matching problem by using a recent PC with much enhanced computational power in 2005, and found that the coefficient matching method works well for most practical cases [24], [27]. They tried up to $N = 6$ cases. They also investigated into the order of zeros in conjunction with element value spread, and discovered that the element value spread become minimum for a particular order of zero sequence within the same transfer function.

There certainly do exist many numerical circuit optimization experiences directly applied to RCPF circuits; however, they are kept inside designer's company and are seldom reported. By the author's experience, it actually works. But, it takes much longer time to converge than simple coefficient matching technique applied to transfer function.

4.2 Coefficient Matching Technique

The transfer function from the circuit analysis result is given by Eq. (12) or (13) must coincide with the designed transfer function, for example, Eq. (19) with Eqs. (20) and (21).

After expanding denominator polynomial of Eq. (12), we have

$$H_C(s) = \frac{(1-\mathrm{j}sC_1R_1)(1-\mathrm{j}sC_2R_2)\cdots(1-\mathrm{j}sC_2R_2)}{b_N s^N + \cdots + b_2 s^2 + b_1 s + b_0}, \quad (45)$$

where b_k ($k = 1, 2, \ldots, N$) is a function of all the element values, i.e., $b_k = b_k(C_1, C_2, \ldots, C_N, R_1, R_2, \ldots, R_N)$. In particular, $b_0 = 1$ and $b_N = \tau_1^{[p]} \ldots \tau_N^{[p]}$ hold. Here, C_k and R_k denote the k-th stage capacitor and resistor values, and those are what we are seeking for.

On the other hand, transfer function designed by direct design method is represented by

$$H_D(s) = \frac{(1-\mathrm{j}s\tau_1^{[z]})(1-\mathrm{j}s\tau_2^{[z]})\cdots(1-\mathrm{j}s\tau_N^{[z]})}{a_N s^N + \cdots + a_2 s^2 + a_1 s + a_0}. \quad (46)$$

Here, a_k ($k = 1, 2, \ldots, N$) are real coefficients of the denominator polynomial. Equating the coefficients of numerators and denominators of Eq. (45) and Eq. (46), we have the following relation in order they have the same response:

$$\tau_m^{[z]} = C_k R_k, \text{ and } a_m = b_k \quad (47)$$

for $m, k = 1, 2, \ldots, N$.

Note that $m = k$ is not necessarily required for all $k = 1, 2, \ldots, N$. This allows the change of zero removal order by letting $m \neq k$ for some k. So, there are $N!$ of zero orders in total. The order of zero removal has a great impact on element value spread. This topic will be explained in the design example 6.

For Butterworth and equal ripple RCPFs, poles of $H_D(s)$ have symmetry relations of Eqs. (24)–(27), then, always $a_0 = 1$ and $a_N = \prod_{k=1}^{N} C_k R_k = 1$ hold. This means that

†They assumed that the realized order of zeros are fixed in ascending order of their magnitude.

$a_N = b_N$ must be excluded from the condition, and we have only $2N-1$ equations for $2N$ unknown RC values. This is overcome by setting $R_1 = 1$ without loss of generality, and we can solve the simultaneous equations. If necessary, R_1 may be changed to any value by applying impedance scaling on the resulting element values.

For those transfer functions that do not have the above symmetry properties, i.e., $a_0 \neq 1$ and/or $a_N \neq 1$, it is clear that $H_C(s)$ and $H_D(s)$ will never match. Such a transfer function implies that the source resistance and/or output termination exist, and is obviously not realizable by simply cascading basic RCPF sections. It is known that some of such cases can be solved similarly by the coefficient matching technique after incorporating a source resistance and a load resistance [29].

It is difficult, in practice, to find numerically the roots of the nonlinear simultaneous equations of Eq. (47), we may define an equivalent numerical minimization problem and solve it instead. For example, we may use the least square method and minimize M:

$$M = \sum_{m,k=1}^{N} (\tau_m^{[z]} - C_k R_k)^2 + \sum_{m,k=1}^{N-1} (a_m - b_k)^2 \tag{48}$$

with respect to C_k, R_k values assuming $R_1 = 1$.

(1) *Design example 5*: Exact solution ($N = 2$)

We realize $N = 2$ equal ripple RCPF in this example. The transfer function from the circuit analysis is given by

$$H_{C2}(s) = \frac{(1-\mathrm{j}sC_1R_1)(1-\mathrm{j}sC_2R_2)}{b_2 s^2 + b_1 s + b_0}, \tag{49}$$

$$b_2 = C_1 C_2 R_1 R_2, \tag{50}$$

$$b_1 = C_1 R_1 + 2C_2 R_1 + C_2 R_2, \tag{51}$$

$$b_0 = 1. \tag{52}$$

The normalized voltage transfer function of equal ripple type RCPF has the symmetry property of Eqs. (26) and (27), $\tau_1^{[p]}\tau_2^{[p]} = \tau_1^{[z]}\tau_2^{[z]} = 1$ must hold. Then, we have the following expression.

$$H_{D2}(s) = \frac{(1 - \mathrm{j}s\tau_1^{[z]})(1 - \mathrm{j}s/\tau_1^{[z]})}{(1 + s\tau_1^{[p]})(1 + s/\tau_1^{[p]})} \tag{53}$$

Therefore, the coefficient matching method yields the following conditions:

$$\tau_1^{[z]} = C_1 R_1, \quad 1/\tau_1^{[z]} = C_2 R_2, \tag{54}$$

$$b_2 = C_1 R_1 C_2 R_2 = 1, \quad b_0 = 1, \tag{55}$$

$$b_1 = C_1 R_1 + 2C_2 R_1 + C_2 R_2 = \tau_1^{[p]} + 1/\tau_1^{[p]}. \tag{56}$$

Eliminating redundant conditions (Eq. (55)) and solve for C_1, C_2, R_2 with $R_1 = 1$, the element values are exactly calculated for equal-ripple design, as [4]:

$$R_1 = 1, \; C_1 = \tau_1^{[z]}, \; R_2 = \frac{2}{\tau_1^{[z]}\left(\tau_1^{[p]} + \frac{1}{\tau_1^{[p]}} - \tau_1^{[z]} - \frac{1}{\tau_1^{[z]}}\right)}, \tag{57}$$

Table 4 Design example for $N = 4$ equal-ripple RCPF [27].

Zeros: $\lvert z_k \rvert$	0.350199, 0.663872, 1.50632, 2.85552		
Poles: $\lvert p_k \rvert$	0.151395, 0.597022, 1.67498, 6.60526		
Sequence of zeros	(1234)	(2413)	(2314)
R_1	1.0000E+00	1.0000E+00	1.0000E+00
R_2	1.6838E+00	1.4103E+00	4.2704E+00
R_3	3.2328E+00	7.2402E+00	1.5647E+01
R_4	5.4433E+00	1.0211E+01	1.0330E+01
C_1	2.8555E+00	1.5063E+00	1.5063E+00
C_2	8.9460E−01	2.4832E−01	1.5546E−01
C_3	2.0536E−01	3.9440E−01	1.8249E−01
C_4	6.4335E−02	6.5018E−02	3.3900E−02
R_{max}/R_{min}	5.4433E+00	1.0211E+01	1.5647E+01
C_{max}/C_{min}	4.4385E+01	2.3167E+01	4.4434E+01
Spread M_1	4.9828E+01	3.3378E+01	6.0081E+01

$$C_2 = \frac{1}{2}\left(\tau_1^{[p]} + \frac{1}{\tau_1^{[p]}} - \tau_1^{[z]} - \frac{1}{\tau_1^{[z]}}\right). \tag{58}$$

As seen from the above, $N = 2$ case has an exact solution for equal ripple design. If necessary, value of R_1 may be changed by applying impedance scaling on the resulting element values.

Recently, Hata et al. obtained exact solutions for Butterworth RCPFs up to $N = 4$ case by the coefficient matching method [25], [26].

(2) *Design example 6*: Coefficient matching ($N = 4$) [27]

Normalized transfer function of an RCPF with $N = 4$ and $\omega_L/\omega_H = 1/10$ was designed by the direct method. Obtained poles and zeros are listed on top of Table 4. Then, coefficient matching was performed via least square method with all the possible order of zeros. Eight cases were not converged out of total $4! = 24$ cases. Non-convergent zero orders are (1243), (1324), (2134), (2143), and their reverse orders, from input side to output side.

A measure for element value spread, M_1, is defined as a sum of maximum resistor value spread and maximum capacitor value spread within the realized circuit:

$$M_1 = \frac{R_{max}}{R_{min}} + \frac{C_{max}}{C_{min}}. \tag{59}$$

By the definition, M_1 is invariant to impedance scaling and frequency scaling, and is a good measure of element value spread. The smallest three cases for M_1 are shown in Table 4 together with resulted element values.

Table 4 indicate that the sequence of zeros (2413) gave the smallest M_1. This clearly shows that sequence of zeros and element value spread are strongly related. However, it is not known what zero order gives the minimum element value spread prior to realizing the RCPF.

4.3 Cascade Synthesis of RCPFs

By introducing additional shunt branches of capacitor or resistor in between RCPF sections, McGee proposed a cascade synthesis procedure specialized for RC polyphase networks for given transadmittance y_{21} and driving point admittance y_{22} [30]. However, he did not clarify what class of transfer functions can be realized by the procedure.

Recently, Nishi et al. tackled with this problem and proved that the transfer function with all the zeros are concentrated at the identical point can be realized without shunt capacitors or resistors, under some mild condition [31], [32]. This corresponds to Butterworth type RCPFs. For general case with distributed transmission zeros, only a loose sufficient condition for the realizability was obtained [31]. However, neither necessary and sufficient condition, nor tight sufficient condition is known for a transfer function to be realized by the procedure to date.

Nevertheless, the synthesis procedure seems to work well for many practical problems [35]. This section sketches an outline of the cascade synthesis and some of its applications.

4.3.1 Synthesis of Real *RC* 2-Ports

Before going into cascade synthesis of RCPF, we take a quick review of real *RC* 2-ports synthesis form given transfer function [33].

Open circuit voltage transfer function $T_{\mathrm{V}}(s)$ of a circuit having admittance matrix driven by a voltage source is given by:

$$T_{\mathrm{V}}(s) = -\frac{y_{21}(s)}{y_{22}(s)}. \tag{60}$$

We would like to find y_{21} and y_{22} having a common denominator polynomial $h(s)$. Then, y_{21}, y_{22} of Eq. (60) must be of the following form [33]:

$$-y_{21}(s) = \frac{Q(s)}{h(s)}, \;\; y_{22}(s) = \frac{P(s)}{h(s)}. \tag{61}$$

This implies that the transmission zeros are originated from that of $y_{21}(s)$, and poles are originated from the zeros of $y_{22}(s)$. The common denominator polynomial $h(s)$ may be arbitrary, as far as Eq. (61) can be physically realized; however, it is not determined by only given the transfer function. To determine $h(s)$, we make use of the following conditions for *RC* driving point admittance y_{22} to satisfy:

1. All the zeros and poles of an *RC* driving point admittance exist on the negative real axis including $s = 0$ and $s = \infty$, and that
2. they are all simple and poles and zeros are interleaved each other, and that
3. the nearest one to the origin is a zero.

The polynomial $h(s)$ may be arbitrarily chosen so as to meet the above conditions; although element values and attenuation of the realized circuit will be different depending on how $h(s)$ is chosen. This problem of how to chose optimum $h(s)$ for real *RC* circuits is not solved to the best knowledge of the author [34], and this is true for RCPFs.

On the other hand, zeros of y_{21}, i.e., polynomial $Q(s)$, can be anywhere of the s-plain.

In the RCPF synthesis, poles of the driving point admittance are restricted on the negative real axis as in the case of real *RC* circuits. Unlike real *RC* circuits, zeros are restricted on the negative (or positive) imaginary axis. In addition, RCPF circuits are non-reciprocal. Those points hinder direct application of the conventional *RC* circuit synthesis procedure. Keeping those in mind, see how cascade synthesis of RCPFs proceeds in the next section.

4.3.2 Outline of Cascade Synthesis of RCPFs

McGee's procedure synthesizes an RCPF circuit, for a given voltage transfer function, by using unit RCPF sections with shunt arms consisting of only a resistor or a capacitor. The procedure realizes RCPF circuit from driving point admittance and zeros by using zero shifting technique.

Voltage transfer function of n-stage RCPF is already obtained by the Eq. (12). Driving point admittance $y_{22}(s)$, which is needed for synthesis, is obtained by assigning it zeros with poles of the transfer function, and finding appropriate poles p_k $(k = 1, 2, \dots n-1)$ as:

$$y_{22}(s) = \frac{(s - 1/\tau_1^{[\mathrm{p}]})(s - 1/\tau_2^{[\mathrm{p}]})\dots(s - 1/\tau_n^{[\mathrm{p}]})}{(s - p_1)(s - p_2)\dots(s - p_{n-1})}. \tag{62}$$

The unit RCPF section to be extracted must have a shunt admittance y (a conductance g or a capacitance c) at its output side in order to apply zero shift technique (see Fig. 8, top). Resulted circuit will be an n-cascaded version of the g (or c) loaded unit sections. The k-th section has an admittance matrix $\boldsymbol{Y}_k$ of the form:

$$\boldsymbol{Y}_k = \begin{pmatrix} G_k(1 + s\tau_k^{[\mathrm{z}]}) & -G_k(1 + \mathrm{j}s\tau_k^{[\mathrm{z}]}) \\ -G_k(1 - \mathrm{j}s\tau_k^{[\mathrm{z}]}) & G_k(1 + s\tau_k^{[\mathrm{z}]}) + y_k \end{pmatrix}. \tag{63}$$

Here, $\tau_k^{[\mathrm{z}]} \equiv C_k R_k$, $G_k = 1/R_k$ and $y_k(g_k$ or $sc_k)$ is a shunt conductance (or capacitance) at k-th unit section output. Then, if we know G_k and y_k, all the element values in k-th unit section can be determined.

Figure 8 shows the procedure to extract each unit section form output side to input side, where Y_1 is a driving point admittance of the section to be extracted looking from output side, and Y_2 is a driving point admittance looking into the rest of the circuit from the output side. The circuit is realized in such a way that the extracted unit section has a desired zero, by forcing the circuit to have $y_{21}(s)$ with zero

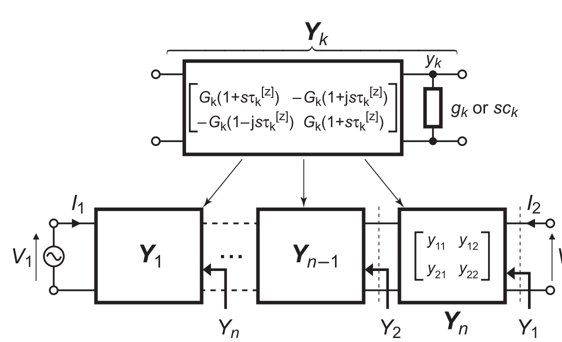

Fig. 8 Cascade synthesis procedure.

shifting technique. The remaining Y_2 has a degree lower than that of Y_1 by one, after a unit section is extracted. By repeated application of this procedure, it terminates if $Y_2 = \infty$ (shorted by an input voltage source) is established.

Now, the output admittance, Y_1, of a circuit characterized by $\boldsymbol{Y} = [y_{ij}]$ driven by a signal source admittance of Y_2 is given by the next expression:

$$Y_1 = \frac{-y_{12}y_{21}}{y_{11} + Y_2} + y_{22}. \tag{64}$$

We begin the cascade synthesis with this expression from the output side, i.e., n-th stage, toward the input side.

From Eq. (63), transadmittance from the output side to the input side direction is given by $y_{12}(s) = -G_n(1 + \mathrm{j}s\tau_n^{[z]})$, and thus, $y_{12}(\mathrm{j}/\tau_n^{[z]}) = 0$ must hold, for its zero exists at $s = \mathrm{j}/\tau_n^{[z]} = z_k^{*\dagger}$. Then, y_{22} of the n-th stage can be extracted as $y_{22}(z_n^*) = Y_1(z_n^*) = G_n(1 + \mathrm{j}) + y_n$, because the preceding sections are not seen from right side of $\boldsymbol{Y}_n$ at the transmission zero frequency. Here, y_n is added in order $Y_1(z_n^*)$ to have equal real part and imaginary part. This determines all the element values in the n-th stage, and enables us to calculate Y_2 as a remaining driving point admittance, as updated Y_1, by solving Eq. (64) for Y_2, then we can proceed to the next step, the $(n-1)$-st stage, and continue the synthesis procedure.

The algorithm for finding k-th section parameters G_k and y_k is as follows. The k-th section is extracted by evaluating input admittance Y_1 at $s = z_k^*$:

$$Y_1(z_k^*) = G_k(1 + \mathrm{j}) + y_k, \tag{65}$$

where,

$$G_k = \max\left\{\mathrm{Re}\left[Y_1(z_k^*)\right], \mathrm{Im}\left[Y_1(z_k^*)\right]\right\}, \tag{66}$$

$$y_k = \begin{cases} g_k & \text{if } g_k > 0 \\ \mathrm{j}c_k = \mathrm{j}\left(-g_k/\tau_k^{[z]}\right) & \text{if } g_k < 0 \end{cases}, \tag{67}$$

$$g_k = \mathrm{Re}[Y_1(z_k^*)] - \mathrm{Im}[Y_1(z_k^*)]. \tag{68}$$

(1) *Design example 7*: Cascade synthesis [30]

Suppose we want to realize the voltage transfer function

$$H(s) = \frac{(1 - \mathrm{j}s)(1 - \mathrm{j}s/2)}{(1 + s)(3 + s)}. \tag{69}$$

Note that this is neither Butterworth nor equal ripple type transfer function, and that this $H(s)$ cannot be realized by conventional cascaded RCPF sections, because $H(0) \neq 1$.

Using the poles and zeros of $H(s)$, we specify transadmittance y_{21} and input admittance $Y_1(= y_{22})$ as

$$y_{21}(s) = \frac{(1 - \mathrm{j}s)(1 - \mathrm{j}s/2)}{2 + s}, \tag{70}$$

$$Y_1(s) = y_{22}(s) = \frac{(1 + s)(3 + s)}{2 + s}, \tag{71}$$

and realize them simultaneously. The common denominator $h(s) = b + s$ is determined in such a way that poles and zeros of Y_1 are interleaved each other. This restricts b to be between 1 and 3, and $b = 2$ is adopted arbitrarily. Thus, Y_1 is a driving point admittance of an *RC* circuit.

Since zeros of y_{21} are at $s = -\mathrm{j}, -\mathrm{j}2$, the zeros of y_{12} are at $s = \mathrm{j}, \mathrm{j}2$. Here, we extract $s = \mathrm{j}$, first. $Y_1(\mathrm{j})$ can be decomposed as;

$$Y_1(\mathrm{j}) = \frac{(1 + \mathrm{j})(3 + \mathrm{j})}{2 + \mathrm{j}} = \frac{8}{5} + \mathrm{j}\frac{6}{5} = \frac{6}{5}(1 + \mathrm{j}) + \frac{2}{5}, \tag{72}$$

because $\tau_1^{[z]} = 1$. This can be represented as $Y_1(\mathrm{j}) = g_2 + G_2(1 + \mathrm{j})$, and $g_2 = 2/5$, $G_2 = 6/5$, $C_2 = 6/5$. Then, the admittance matrix of this section, $\boldsymbol{Y}_2$, will be

$$\boldsymbol{Y}_2 = \begin{pmatrix} \frac{6}{5}(1 + s) & -\frac{6}{5}(1 + \mathrm{j}s) \\ -\frac{6}{5}(1 - \mathrm{j}s) & \frac{6}{5}(1 + s) + \frac{2}{5} \end{pmatrix}. \tag{73}$$

The input admittance, Y_2, after removing the section can be obtained by solving Eq. (64) for Y_2:

$$Y_2 = \frac{y_{12}y_{21}}{y_{22} - Y_1} - y_{11} = 6s + \frac{66}{5} \tag{74}$$

Therefore, the rest section can be extracted by evaluating the input admittance,Y_2, at the second zero $z_2^* = \mathrm{j}2$ or $\tau_2^{[z]} = 1/2$ as above. We have

$$Y_2(\mathrm{j}2) = \mathrm{j}12 + \frac{66}{5} = 12(1 + \mathrm{j}/2) + \frac{6}{5}. \tag{75}$$

This corresponds to $G_1 = 12$, $C_1 = 6$, $g_1 = 6/5$, and the next section is extracted as:

$$\boldsymbol{Y}_1 = \begin{pmatrix} 12(1 + s/2) & -12(1 + \mathrm{j}s/2) \\ -12(1 - \mathrm{j}s/2) & 12(1 + s/2) + \frac{6}{5} \end{pmatrix}. \tag{76}$$

Then, the next input admittance, Y_3, is given by

$$Y_3 = \frac{y_{12}y_{21}}{y_{22} - Y_2} - y_{11}. \tag{77}$$

Since $y_{22} = Y_2$, the denominator polynomial is zero, and $Y_3 = \infty$. Thus, the synthesis procedure terminates.

The actually realized transfer function, $H(s)'$, is calculated from the obtained element values to be

$$H(s)' = \frac{(1 - \mathrm{j}s)(1 - \mathrm{j}s/2)}{(1 + s)(3 + s)} \times 2, \tag{78}$$

and this confirms that the desired transfer function is realized within a constant gain multiplier of 2. The realized circuit is shown in Fig. 9. Its dc gain is 2/3, and this is attributed to shunt resistors newly introduced by McGee's method. Sum of element value spread $M_1 = 30.2$ for this design.

(2) *Design example 8*: Change zero extraction order [35]

We realize the same transfer function of the previous example, Eq. (69), to illustrate the method to change the order of

†Note that $y_{12} \neq y_{21}$ for RCPFs, i.e., non-reciprocal.

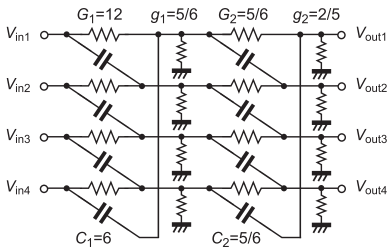

Fig. 9 Realized RCPF for example 7.

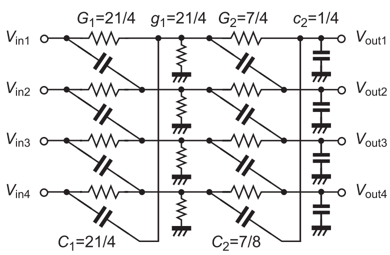

Fig. 10 Realized RCPF for example 8.

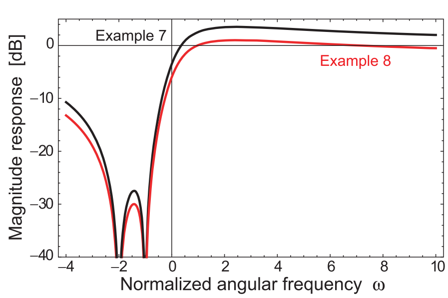

Fig. 11 Effect of zero extraction order.

zero extraction.

This time we extract zero at $s = \mathrm{j}2$ first. The input admittance is calculated to be $Y_1(\mathrm{j}2) = 7/4 + \mathrm{j}\,9/4$; however, the imaginary part is larger than the real part. So, we use a shunt capacitor c_2, instead of a shunt conductor for zero shifting. That is, decompose Y_1 as $Y_1(\mathrm{j}2) = 7/4(1 + \mathrm{j}) + \mathrm{j}/2$ and obtain $G_2 = 7/4$, and $C_2 = 7/8$. The shunt capacitor c_2 has a susceptance of $\mathrm{j}/2$ at $\omega = 2$, then, its element value is $c_2 = 1/4$ as calculated by Eq. (67).

Now, the element values are substituted into Eq. (74), and we obtain $Y_2 = 21/4 \times (2 + s)$. This is evaluated at $s = \mathrm{j}$, the second zero, we have $Y_2(\mathrm{j}) = 21/2 + \mathrm{j}21/4 = 21/4 \times (1 + \mathrm{j}) + 21/4$. Then, $G_1 = 21/4$, $C_1 = 21/4$, and $g_1 = 21/4$ follows. Realized RCPF circuit is shown in Fig. 10.

Realized transfer function, $H(s)''$, is calculated from the obtained element values to be

$$H(s)'' = \frac{(1 - \mathrm{j}s)(1 - \mathrm{j}s/2)}{(1 + s)(3 + s)} \times \frac{3}{2}. \tag{79}$$

The constant multiplier of 3/2 is less than the former design, and shows larger attenuation over frequencies. This indicates that the zero extraction order of former design is preferable in most cases (see Fig. 11).

Sum of element value spread is calculated to be $M_1 = 24$ for this design. This is about 80% of the previous design. There are tendency to have smaller M_1 for smaller dc gain among designs with different zero extraction orders by the author's experience [35].

4.4 Remarks on McGee's Cascade Synthesis Method

The following issues are found in the cascade synthesis method.

1. It is not well understood what class of poles and zeros are realized by the cascade synthesis method.
2. The synthesis procedure requires a common denominator polynomial $h(s)$ of y_{21} and y_{22}, which cannot be uniquely determined from a given transfer function alone.
3. Parallel conductance (or capacitance) may be added in between unit RCPF sections. This addition increases freedom of realizable transfer functions; however, attenuation in passband increases.

The first issue is still open. The second issue is related to the third one, because we have possibility to eliminate the shunt conductor (capacitor) by some proper choice of $h(s)$. Also, gain constant of the realized RCPF depends on the choice of $h(s)$, as seen in the design examples 7 and 8.

Kobayashi et al. obtained the *sufficient* condition for a RCPF to be synthesized without adding any shunt arms for Butterworth type RCPF [35]. The condition for such $h(s)$ is to have symmetry of the form [35]:

$$h(s) = (s + b_{N-1})(s + b_{N-2}) \ldots (s + b_2)(s + b_1), \tag{80}$$

$$b_k b_{N-k} = 1 \ \text{ for } \ k = 1, 2, \ldots, N - 1. \tag{81}$$

However, proper choice of b_k is still not known to date, and gain constant depends on the choice of b_k's.

An attempt using the freedom of pole allocation in $h(s)$ to minimize element value spread was reported for Butterworth type RCPFs [35]. They reported that addition of shunt arms reduce element value spread drastically in many cases at the cost of reduced gain constant [35].

Kobayashi et al. also extended the McGee's synthesis method to accommodate finite resistive termination, and parasitic capacitors for each stage [36]. In place of the original method Eq. (65), they introduced virtual extraction of capacitor-conductor parallel circuit based on the identity

$$Y_1(z_k^*) = (G_k - g_k')(1 + \mathrm{j}) + g_k'(1 + \mathrm{j}) + y_k. \tag{82}$$

This indicates that we are always able to extract a parallel circuit of $(g_k' \,\|\, \mathrm{j}g_k')$, whenever $G_k > g_k'$ holds. This enables to extract capacitive shunt arm for each RCPF stage, we may regard them as parasitic capacitors for each stage. They applied this technique to compensate for bottom plate parasitic capacitors which are used in a three-stage equal-ripple RCPF of $\omega_{\mathrm{H}}/\omega_{\mathrm{L}} = 10$, assuming 10% parasitic capacitances of each capacitor. The result is perfect except gain reduction of 4.0 dB in gain constant, when compared to the RCPF without parasitic capacitors [35]. This gain reduction is due to the parallel conductances accompanied to parasitic capacitors.

5. Concluding Remarks

In this paper, exact design methods of RCPFs with equal-ripple type and Butterworth type responses are explained for transfer function design and element value design along with some design examples.

The author tried first to treat RCPFs as a subclass of general passive complex constant circuits, but it seems not very successful. Indeed, not very much is known for RCPF synthesis, while general synthesis method is established for passive complex circuits [7].

McGee's cascade synthesis is very useful, but it was very hard for the author to understand. Its explanation given here is a recasted version based on the authors understanding. It is not very well known what kind of transfer function can be realizable by the cascade synthesis method; however, it is still very useful for practical design by the author's experience.

In practical applications, parasitic capacitors degrade the passband to slant. This can be compensated for at the cost of reduced gain by extending the McGee's method [36]. Further applications of the method may be expected.

From on-chip implementation point of view, layout of RCPF is bothersome, particularly in RF applications, because difference in wire lengths among four lines may cause phase error in applications over giga hertz. References [37], [38] may be of readers' help.

The evaluation of the manufactured RCPFs may also be problematic at high frequencies. It is very difficult to generate symmetric 4-phase signals with high precision, and actual performance of the device under test may be corrupted by insufficient precision of the source signals. For such cases, measurement based on superposition principle by using multi-port network analyzer is proposed [39], [40].

The author is very happy if readers are interested in RCPF design, and cope with open problems in this field.

Acknowledgment

The author is grateful Prof. T. Shima of Kanagawa University for providing the opportunity to write this paper. He also thanks to Prof. C. Muto of Nagasaki University and Prof. K. Shouno of Tsukuba University, for their valuable and continual discussion on RCPF design. He is deeply indebted to Prof. T. Nishi of Waseda University for his guidance in realizability of McGee's method. This work was partly supported by Grant-in-Aid for Scientific Research (C) (22560356).

References

[1] F. Behbahani, Y. Kishigami, J. Leete, and A. Abidi, "CMOS mixers and polyphase filters for large image rejection," J. Solid-State Circuits, vol.36, no.6, pp.873–887, June 2001.
[2] S.J. Fang, A. Bellaouar, S.T. Lee, and D.J. Allstot, "An image-rejection down-converter for low-IF receivers," IEEE Trans. Microw. Theory Tech., vol.53, no.2, pp.478–487, Feb. 2005.
[3] M.J. Gingell, "A symmetric polyphase network," British Patents 1174709 and 1174710, Dec. 1969.
[4] M.J. Gingell, The synthesis and application of polyphase filters with sequence asymmetric properties, Ph.D. Thesis, University of London, 1975.
[5] J. Crols and M. Steyaert, "An analog integrated polyphase filter for a high performance low-IF receiver," Symp. VLSI Circuits Dig., pp.87–88, June 1995
[6] S.H. Galal, M.S. Tawfik, and H.F. Ragaie, "On the design and sensitivity of RC sequence asymmetric polyphase networks in RF integrated transceivers," Proc. 1999 IEEE Int. Symp. on Circuits and Systems, pp.II-593–II-597, June 1999.
[7] V. Belevitch, Classical Network Theory, Holden-Day, San Francisco, 1968.
[8] N. Yamaguchi, H. Kobayashi, J. Kang, Y. Niki, and T. Kitahara, "Analysis of RC polyphase filters — High-order filter transfer functions, Nyquist charts, and parasitic capacitance effects," IEICE Technical Report, CAS2002-112, Jan. 2003.
[9] Y. Niki, J. Kang, H. Kobayashi, N. Yamaguchi, and T. Kitahara, "Analysis of RC polyphase filters — Input impedance, output termination, component mismatch effects, flat-passband filter design," IEICE Technical Report, CAS2002-113, Jan. 2003.
[10] J. Kaukovuori, K. Stadius, J .Ryynänen, and K.A.I. Halonen, "Analysis and design of passive polyphase filters," IEEE Trans. Circuits Syst.-I, vol.55, no.10, pp.3023–3037, Oct. 2008.
[11] S. Bekku, Taisyou Zahyou Hou Kaisetsu (Method of symmetrical coordinates explained), Chapt. 15, Ohm-sha, Tokyo, 1928. (in Japanese)
[12] G.R. Lang and P.O. Brackett, "Complex analog filters," Proc. European Conf. Circuit Theory Design, pp.412–419, The Hague, Netherlands, Aug. 1981.
[13] C. Muto, "A new extended frequency transformation for complex analog filter design," IEICE Trans. Fundamentals, vol.E83-A, no.6, pp.934–940, June 2000.
[14] C. Muto, "A polyphase transfer function design based on frequency transformation from prototype LPF," IEICE Trans. Fundamentals, vol.E91-A, no.2, pp.554–556, Feb. 2008.
[15] K. Hori, "Method of designing passive RC complex filter of Hartley radio receiver," Japanese Patent Application (Kokai), P2007-215230A, Aug. 2007.
[16] A.I. Zverev, Handbook of filter synthesis, John Wiley, New York, 1967.
[17] A.V. Oppenheim and R.W. Schafer, Digital Signal Processing, Chapt. 5, Prentice-Hall, New Jersey, 1975.
[18] M. Lutovac, D. Tošič, and B.L. Evans, Filter design for signal processing using MATLAB and Mathematica, Appendix 12, Prentice-Hall, New Jersey, 2001.
[19] M. Vlcek and R. Unbehauen, "Degree, ripple, and transition width of elliptic filters," IEEE Trans. Circuits Syst., vol.36, no.3, pp.469–472, March 1989.
[20] W. Cauer, Synthesis of Linear Communication Networks, vol.II, Appendix 3, pp.738–757, McGraw-Hill Book Company, New York, 1958.
[21] M. Abramowitz and I.A. Stegun, Handbook of Mathematical Functions, Dover Publications, New York, 1972.
[22] K. Wada and Y. Tadokoro, "Approximate design of RC polyphase filters with amplitude characteristics being flat in passbands and equiripple in stopbands," IEICE Trans. Fundamentals (Japanese Edition), vol.J88-A, no.12, pp.1478–1486, Dec. 2005.
[23] K. Wada and Y. Tadokoro, "RC polyphase filter with flat gain characteristic," Proc. IEEE Int. Symp. Circuits Syst., pp. I-537–I-540, Bangkok, Thailand, May 2003.
[24] H. Tanabe and H. Tanimoto, "Design considerations for RC polyphase filters with simultaneously equal ripple both in stop-

band and passband," IEICE Trans. Fundamentals, vol.E89-A, no.2, pp.461–464, Feb. 2006.

[25] Y. Hata and C. Muto, "On second and third order RC polyphase filters with butterworth characteristics," THe Papers of Technical Meeting on Electronic Circuits, IEEJ, ECT-09-041, March 2009. (in Japanese)

[26] Y. Hata and C. Muto, "On fourth order RC polyphase filters with butterworth characteristics," THe Papers of Technical Meeting on Electronic Circuits, IEEJ, ECT-09-101, Oct. 2009. (in Japanese)

[27] H. Tanabe and H. Tanimoto, "Design and element value spread considerations for rc polyphase filters with simultaneously equal ripple both in stopband and passband," IEICE Technical Report, CAS2005-30, Sept. 2005. (in Japanese)

[28] H. Tanabe and H. Tanimoto, "Transfer function preserving transformations on equal-ripple RC polyphase filters for reducing design efforts," IEICE Trans. Fundamentals, vol.E90-A, no.2, pp.333–338, Feb. 2007.

[29] T. Nakagawa, K. Shouno, and H. Tanimoto, "Synthesis of an equiripple doubly-terminated RC polyphase filter," The Papers of Technical Meeting on Electronic Circuits, IEEJ, ECT-12-073, Oct. 2012. (in Japanese)

[30] W.F. McGee, "Cascade synthesis of RC polyphase networks," Proc. 1987 IEEE International Symposium on Circuits and Systems, pp.173–176, Philadelphia, PA, USA, 1987.

[31] T. Nishi, H. Tanimoto, and S. Oishi, "Cascade synthesis of RC polyphase one-ports," Proc. ECCTD 2011, pp.81–84, Linkoping, Sweden, Aug. 2011.

[32] T. Nishi, H. Tanimoto, and S. Oishi, "On the realizability condition of RC polyphase 2-ports," IEICE Technical Report, CAS2011-100, Jan. 2012. (in Japanese)

[33] T. Takebe, T. Shinozaki, and M. Teramoto, Ouyou Kairomou Gaku (Applied Network Theory), Chapt. 2, Asakura Shoten,Tokyo, 1972. (in Japanese).

[34] H. Ozaki, "Necessary and sufficient conditions for *RC* transfer functions," J. Electr. Commun. Eng. of Japan, vol.38, no.1, pp.44–49, Jan. 1955. (in Japanese)

[35] T. Kobayashi and H. Tanimoto, "Some considerations on cascade synthesis of RC polyphase filters," The Papers of Technical Meeting on Electronic Circuits, IEEJ, ECT-09-042, March 2009. (in Japanese)

[36] T. Kobayashi and H. Tanimoto, "Design of RC polyphase filters considering bottom plate parasitic capacitances and termination," The Papers of Technical Meeting on Electronic Circuits, IEEJ, ECT-09-70, June 2009. (in Japanese)

[37] G. Grau, Monolithisch-integrerte Schaltungen für lokale Funknetzwerke bei 5.8 GHz, Ph.D. Thesis, Chapt. 5, pp.152–160, Ruhr-Universität Bochum, 2001.

[38] K. Suzuki, M. Ugajin, J. Kodate, and T. Tsukahara, "2-GHz-band highly accurate on-chip polyphase filters," IEICE Technical Report, ICD2001-101, Sept. 2002. (in Japanese)

[39] K. Shouno and Y. Ishibashi, "A note on the measurement method of the frequency response of a complex coefficient filter," IEICE Trans. Fundamentals (Japanese Edition), vol.J83-A, no.12, pp.1486–1494, Dec. 2000.

[40] J. Onodera, K. Kawabe, and H. Tanimoto, "Measurement of frequency response for fully differential polyphase filters without using quadrature oscillator," The Papers of Technical Meeting on Electronic Circuits, IEEJ, ECT-10-029, March 2010. (in Japanese)

Hiroshi Tanimoto received the B.E., M.E., and Ph.D. degrees in Electronic Eng. all from Hokkaido University, in 1975, 1977, and 1980, respectively. In 1980 he joined the Research & Development Center, Toshiba Corp., Kawasaki, Japan, where he was engaged in research and development of telecommunication LSIs. Since 2000, he has been a Professor in the Dept. of Electrical and Electronic Eng., Kitami Institute of Technology, Kitami, Japan. His main research interests include analog integrated circuit design, analog signal processing, and circuit simulation algorithms. He had been an associate editor for *IEICE Trans. Fundamentals*, *IEEE TCAS-II*, and *IEICE Trans. Electron.* He also served as a guest editor for *IEICE Trans. Fundamentals*, and *IEICE Trans. Electron.* He was the past chair of IEEE Circuits and Systems Society Japan Chapter. He is a TPC chair of 2012 International Conference on Analog VLSI Circuits. Dr. Tanimoto is a member of IEEJ and IEEE.